microorganisms

MDPI

Article

The influence of microbial mats on travertine precipitation in active hydrothermal systems (Central Italy)

Giovanna Della Porta [1]* and Joachim Reitner [2]

[1] Earth Sciences Department, University of Milan, via Mangiagalli 34, 20133 Milan, Italy; giovanna.dellaporta@unimi.it. Orcid 0000-0003-3479-0592

[2] Geobiology, Göttingen Centre of Geosciences, Georg-August-University Göttingen, Goldschmidtstr. 3, 37077 Göttingen, Germany; jreitne@gwdg.de

* Correspondence: giovanna.dellaporta@unimi.it

Received: date; Accepted: date; Published: date

Supplementary Materials

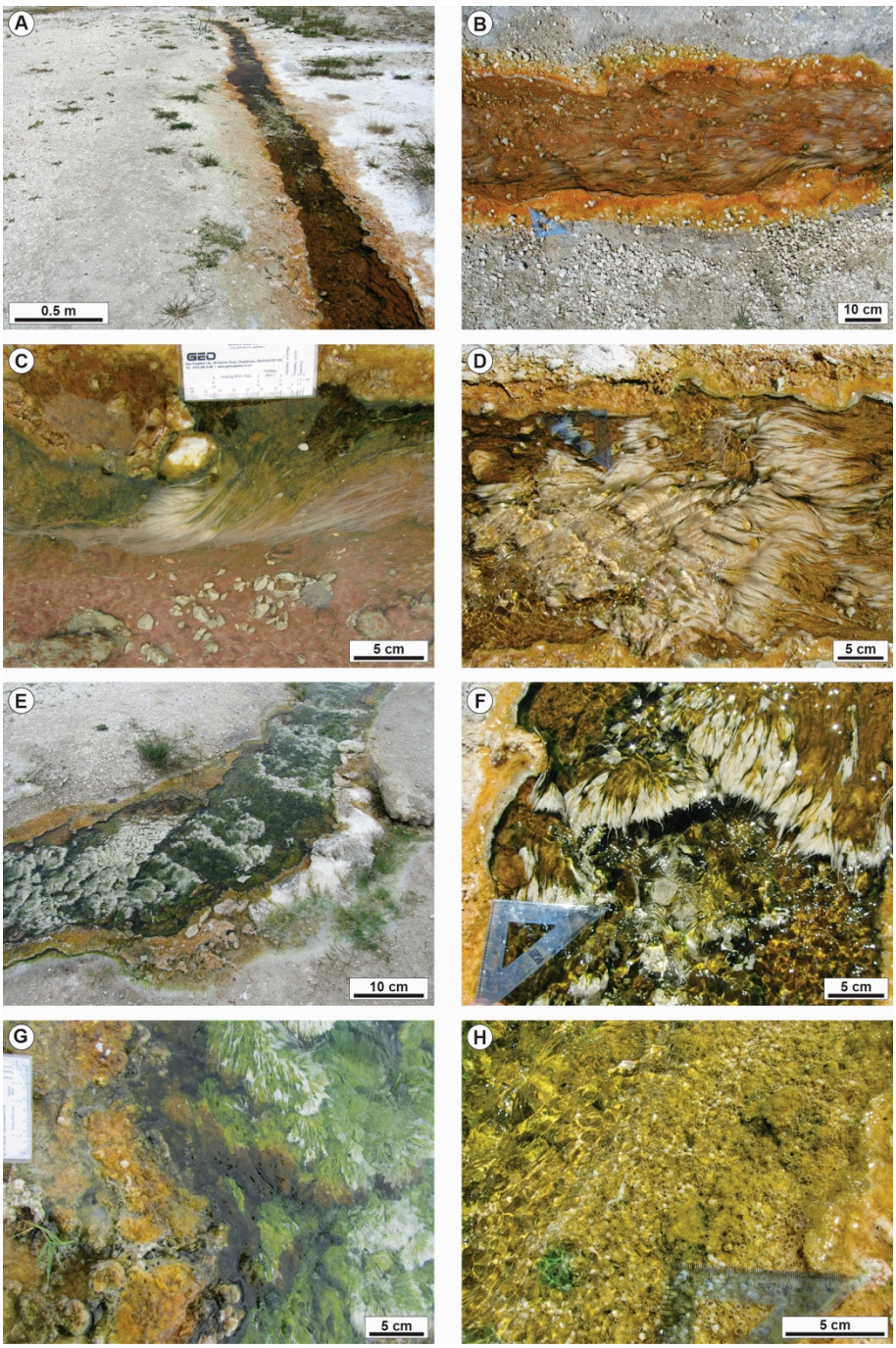

Figure S1. Bullicame (Viterbo) active hydrothermal travertine system. A-B-C) Proximal channel, from 12.5 m to 20 m from the vent centre, draped by purple microbial mats in the centre, with sparse bundles of white filaments oriented according to the current flow direction and with orange/yellow to green microbial mats on the channel margin. D-E-F) Proximal channel in the stretch from 20 m to 40 m from the vent centre with abundant bundles of carbonate-coated filaments, the channel floor draped by microbial mats that change in colour from purple to green while the channel margins are orange/yellow to green in colour with gas bubbles. G) Proximal channel at 30 m from the vent with channel margin characterized by yellow/orange microbial mats with coated gas bubbles and the channel centre rich of white filamentous bundles coated by green to brown microbial mat. H) Distal channel at 60 m from the vent centre, with centre and margin draped by orange/yellow to green microbial mat with abundant carbonate-coated gas bubbles and rafts.

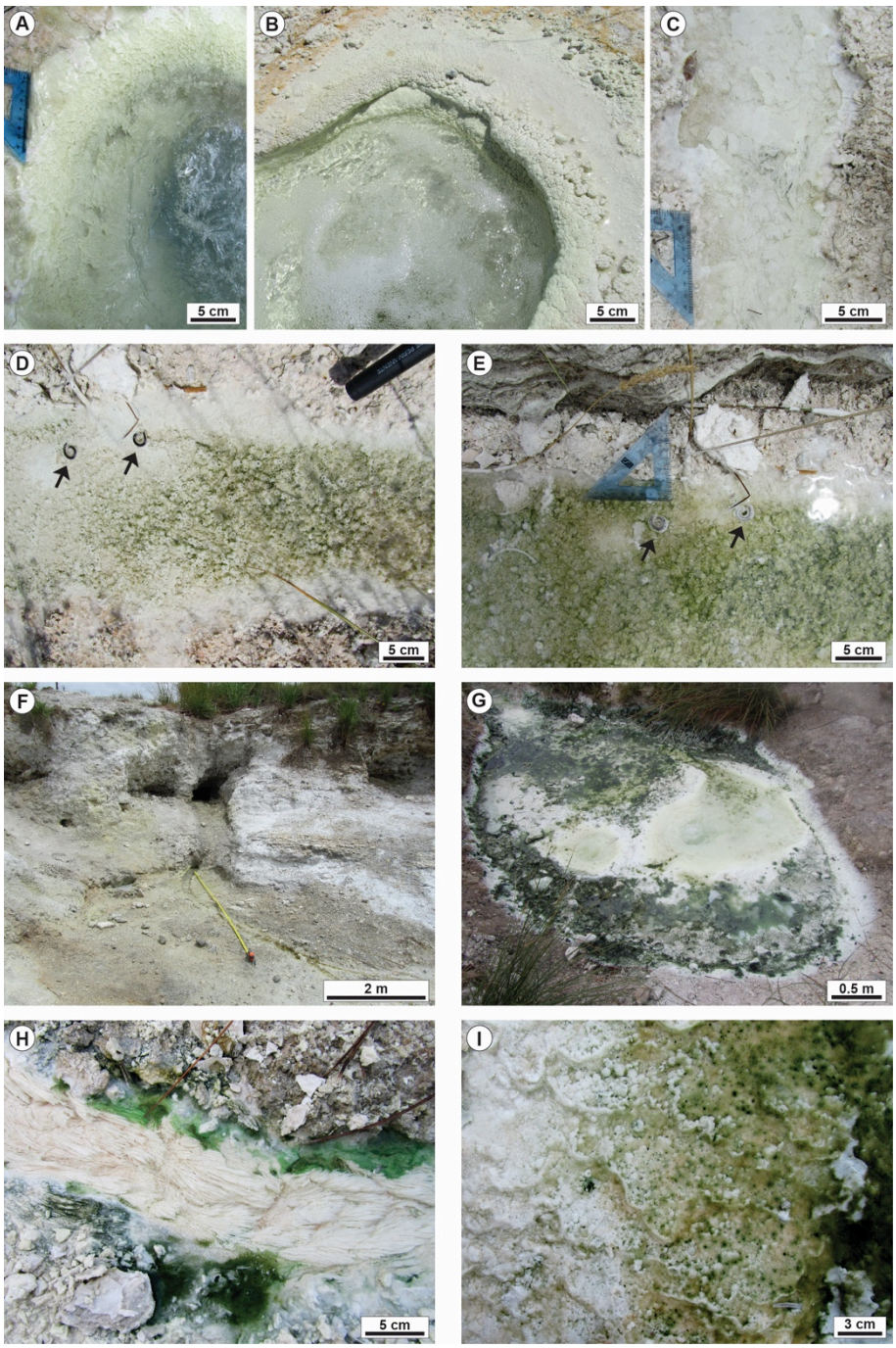

Figure S2. Bollore (Bagni San Filippo) active hydrothermal travertine system. A-B) Close-up views of the vent orifices with the pool rims encrusted by carbonate as coated filaments and dendrites. C) Proximal channel with white carbonate-encrusted bundles of filaments and paper thin rafts. D-E) Distal channel 12 m from the vent with the channel floor draped by green microbial mat with abundant carbonate-coated gas bubbles. The two images where taken during two following days: to notice that the two dead worms (black arrows) are not coated by carbonate in Figure S2D whereas are carbonate-coated in the image in Figure S2E taken the following day. This confirms the fast rates of carbonate precipitation producing millimetres-thick carbonate coatings in 24 hours. F) Second vent and channel in a lower topographic position. The yellow colour of the sediment is provided by abundant sulphur draping the precipitated travertines. G-H-I) During the winter humid season (January), the main Bollore vent and channel thrive with dark green microbial mats, whereas during the summer sampling (July) the green microbial mats were lacking and the channel floor colour was white to light pink.

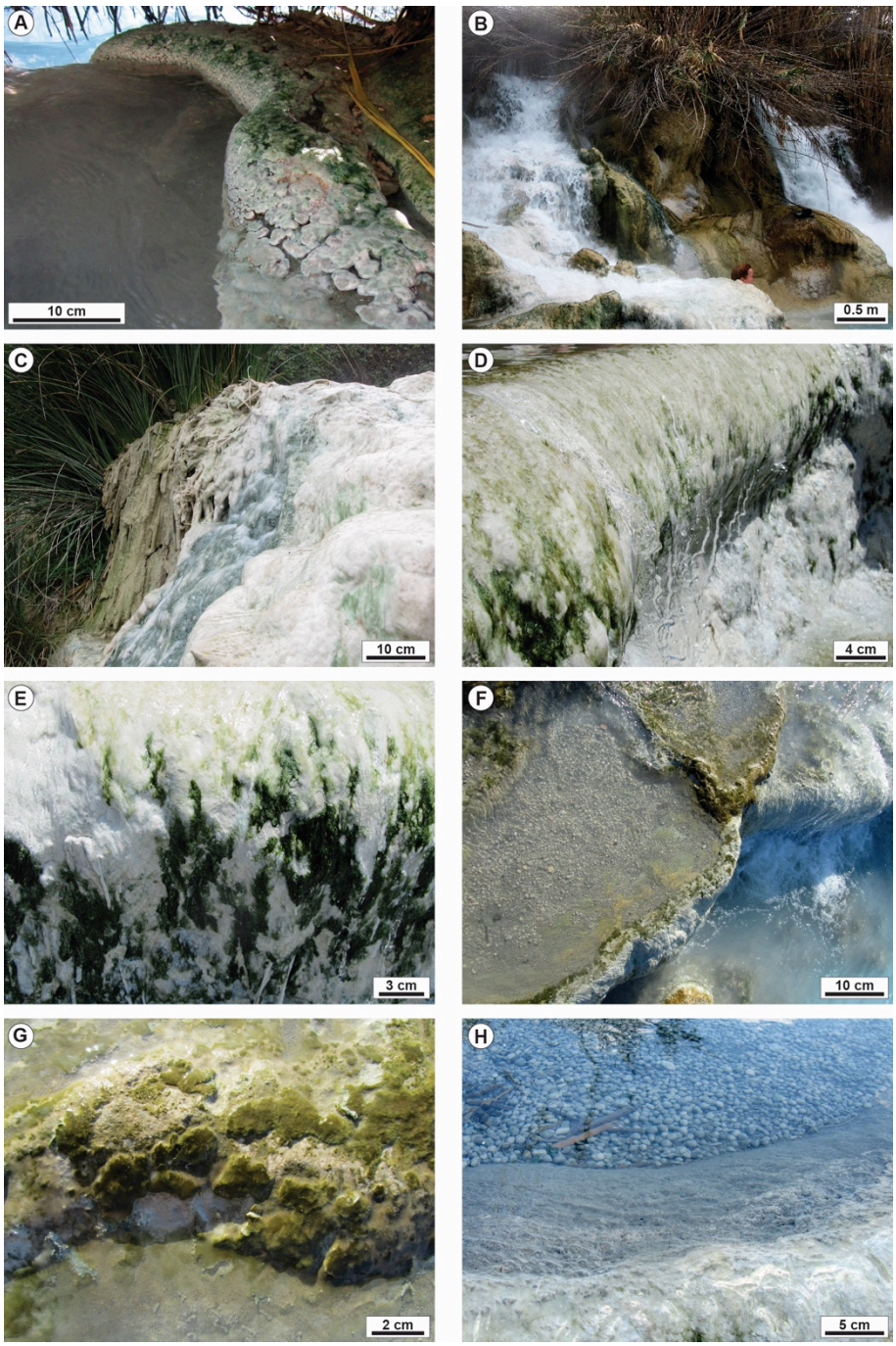

Figure S3. Gorello Waterfall (Saturnia) active hydrothermal travertine system. A) Photograph showing the channel deriving from the thermal spa before the break in slope that generates the waterfall. The channel levees are draped by green to pink microbial mats. B) The nearly 5 m high waterfall developed at the channel topographic break in slope. C) Areas of the pool rims and walls not flooded by thermal water are temporarily colonized by reed vegetation coated by carbonate precipitates when thermal water flow is resumed. D-E) The vertical walls of the pools of the terraced slope are coated by white to dark green microbial mat. F-G) The rims of the pools of the terraced slope are coated by olive green microbial mat. H) Centimetre-size carbonate coated grains (oncoids) forming on the pool floor.

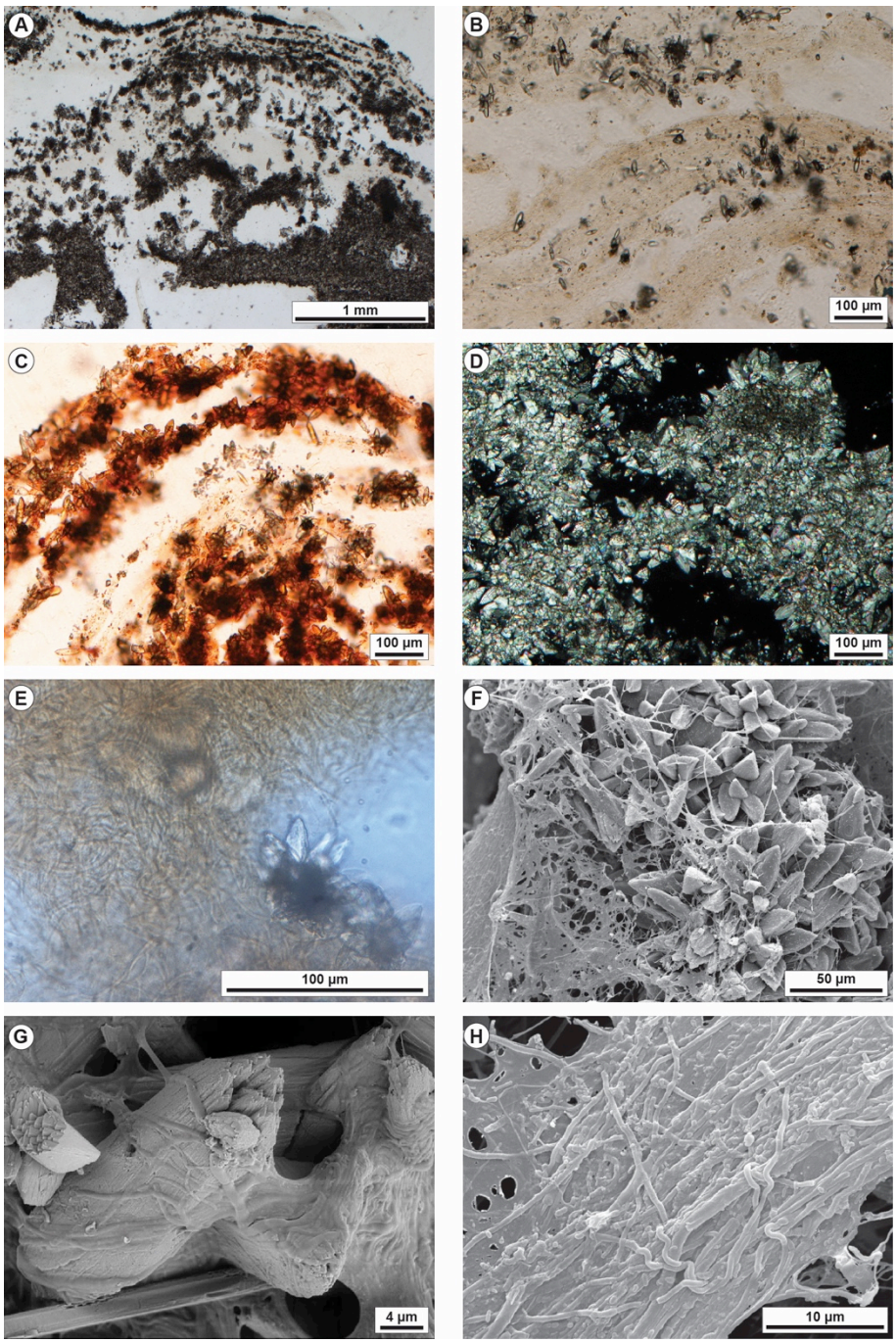

Figure S4. Petrographic and SEM images of the Bullicame travertines in the proximal channel. A) Carbonate precipitates as microsparite/sparite forming spherulites within and above organic substrates. The spatial distribution of the carbonate precipitates forming laminae and irregular mosaics is controlled by the framework of the EPS. B) Calcite crystal spherulites embedded within microbial mat following the shape and geometry of the organic substrate. C) Calcein-dyed sample showing that the calcite crystal spherulites mimic the shape and geometry of the organic substrate binding Ca^{2+} forming undulated laminae. D) Photomicrograph in crossed-polarizers showing the aggregates of microsparite crystals and the sparse clots of micrite mostly at spherulite nuclei. E) Close-up view of calcite spherulites surrounded by filamentous microbes and EPS. F) SEM image showing the rosettes of euhedral prismatic calcite crystals embedded in EPS with filamentous microbes. G) Close-up view at SEM of prismatic calcite crystals embedded in EPS and filamentous microbes. At the bottom a Ca-phosphate crystal. H) SEM image of the microbial mat in the proximal channel consisting of bundles of filamentous microbes. EPS include also rod-shaped microbes (upper left corner).

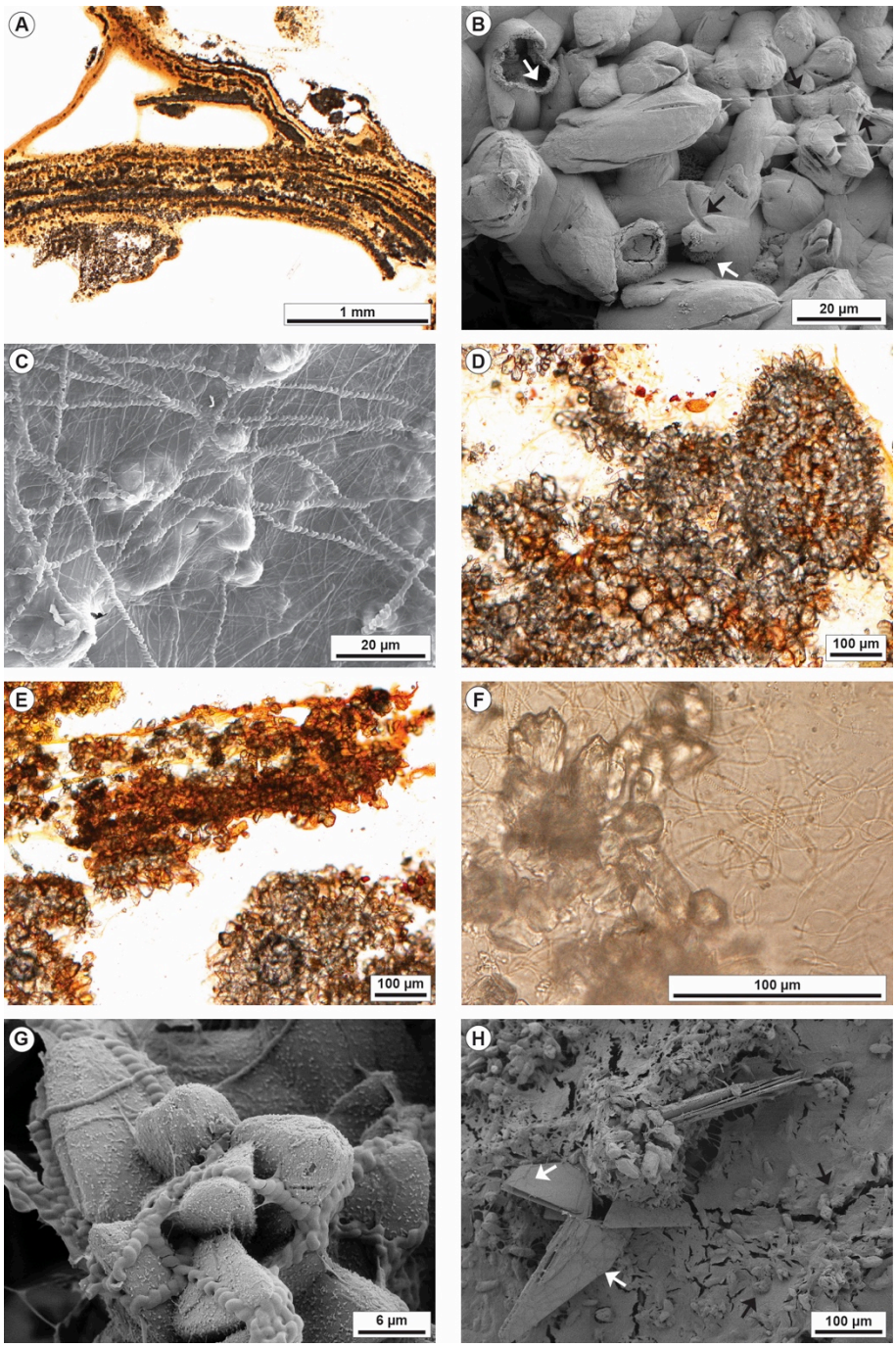

Figure S5. Bullicame travertines in the proximal channel margins (A-C) and distal channel (D-H). A) Tetracycline-dyed sample showing calcite crystal spherulites within the microbial mat following the framework and lamination of the organic substrate. B) SEM image of spindle-shaped microsparite crystals showing tubular perforations likely related to moulds of filamentous microbes entombed during crystal growth with organic filaments emerging from the tubular hollows (black arrows). The image shows also acicular aragonite hollow spheres (white arrows). C) SEM image of EPS surrounding the calcite crystals embedding *Spirulina* cyanobacteria and other filamentous microbes. D) Calcein-dyed sample showing the framework of aggregates of microsparite spherulites associated with micrite clots and laminae. E) Calcein-dyed sample showing the framework of aggregates of microsparite spherulites associated with micrite clots and laminae impregnated by organic matter of the microbial mat. F) Close-up view of the microsparite spherulites with a micrite nucleus surrounded by EPS embedding filamentous microbes including *Spirulina* cyanobacteria. G) SEM image of calcite crystals draped by *Spirulina* cyanobacteria and other filamentous microbes and by a grumous mucilaginous organic material. H) SEM image showing EPS embedding calcite crystals (black arrows) and Ca-phosphate crystals coated by filamentous microbes (white arrows).

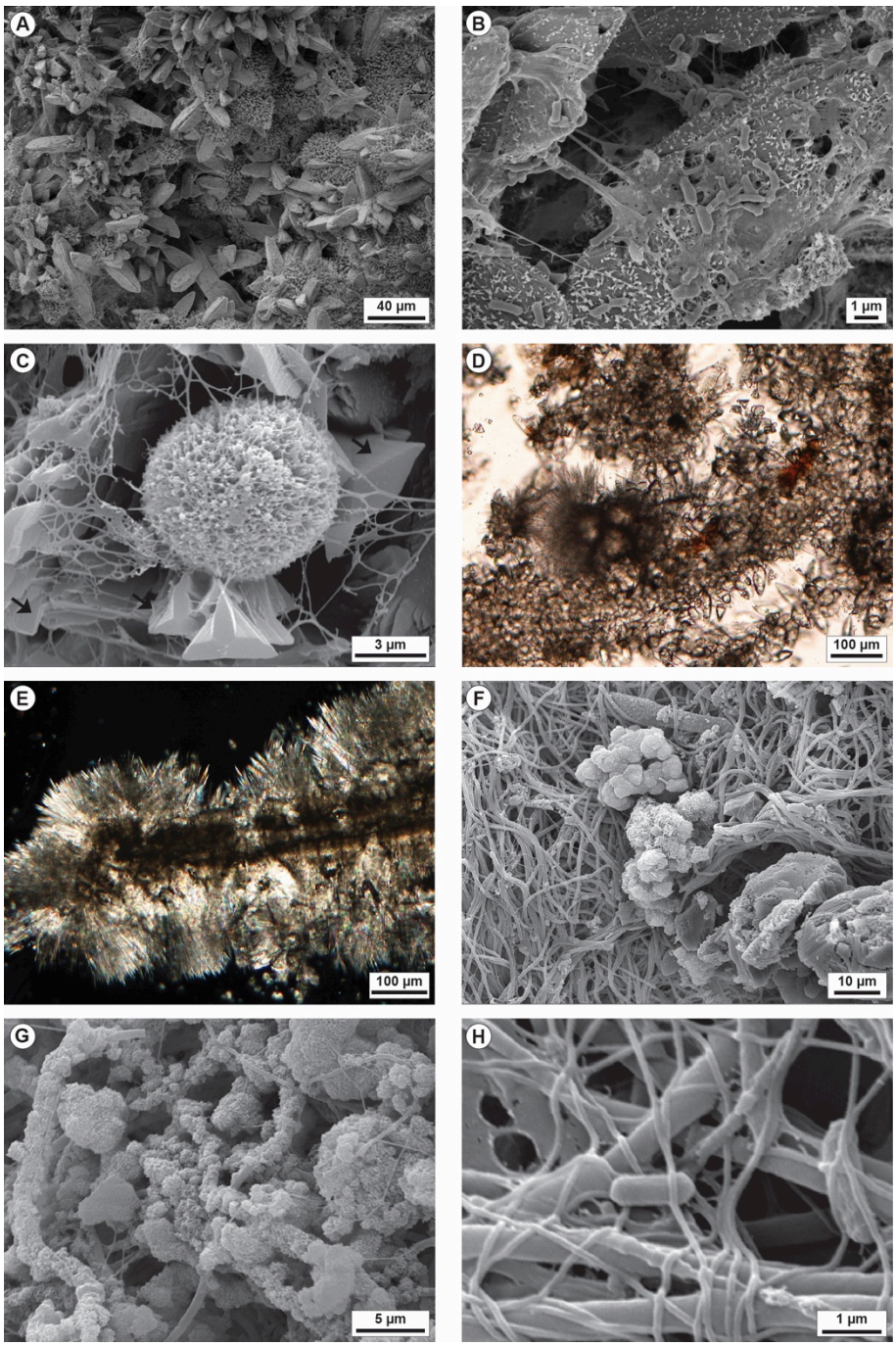

Figure S6. Petrographic and SEM images of the Bollore (Bagni San Filippo) travertines at the main vent (A-C) and second vent (D-H). A) SEM image showing the prismatic calcite crystal forming radial rosettes and the acicular aragonite spherulites that appear to postdate calcite precipitation. B) Calcite crystals embedded in EPS and overlain by rod-shaped microbes. C) SEM image of acicular aragonite spherulites surrounded by gypsum crystals (black arrows) all draped by EPS. D) Carbonate fabric of microsparite spherulites forming aggregates and laminae followed by acicular aragonite spherulites. E) Crossed-polarizers image of micritic and microsparitic laminae surrounded by acicular aragonite crystal fans. F) Bundles of filamentous microbes overlain by aggregates of possible authigenic clay mineral. G) SEM image showing the filamentous microbes coated by authigenic silicate. H) SEM image showing entangled filamentous microbes with different size in cross section and rod-shaped microbes.

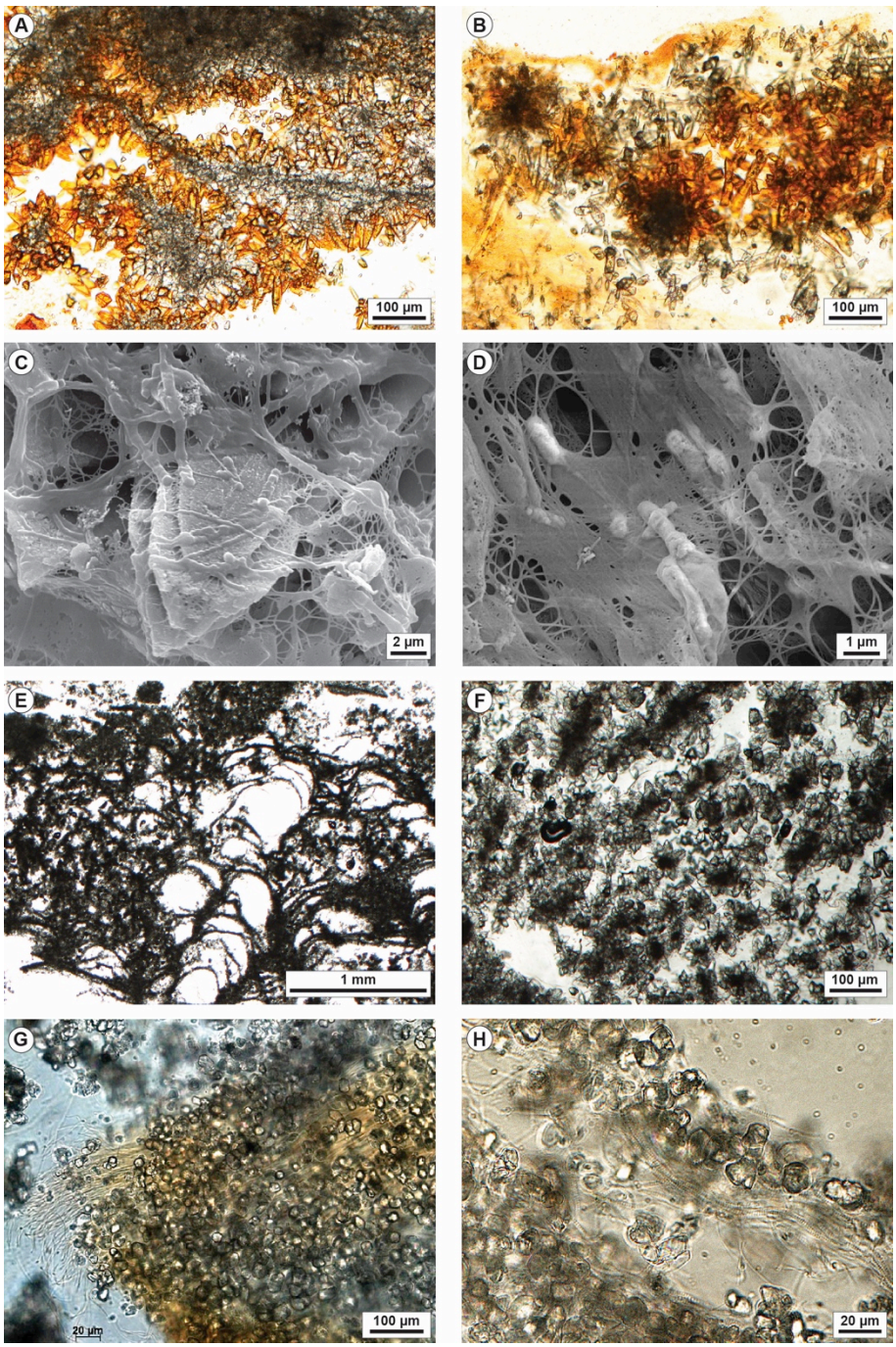

Figure S7. Petrographic and SEM images of the Bollore (Bagni San Filippo) travertines at the proximal (A-D) and distal channel (E-F). A) Micrite filaments and clots surrounded by microsparite to fine sparite crystals departing radially from the micritic substrate. Crystals are stained by orange calcein dye as they were coated by organic matter. B) Calcite crystal spherulites embedded in calcein dyed microbial mat. Some rosettes have the nuclei made of micrite clots. C) SEM image of prismatic calcite crystals with gothic-arch shape surrounded by EPS embedding filamentous and rod-shaped microbes. D) SEM image of EPS embedding rod-shaped microbes. E) Photomicrograph of distal channel coated bubble boundstone made of clotted peloidal micrite. F) Photomicrograph of a framework of calcite crystal spherulites with micrite nuclei aligned and embedded in organic matter that must sustain the crystal framework. G) Microsparite crystals embedded in EPS and filamentous microbes. H) Microsparite crystals surrounded by filamentous microbes with abundant *Spirulina* cyanobacteria.

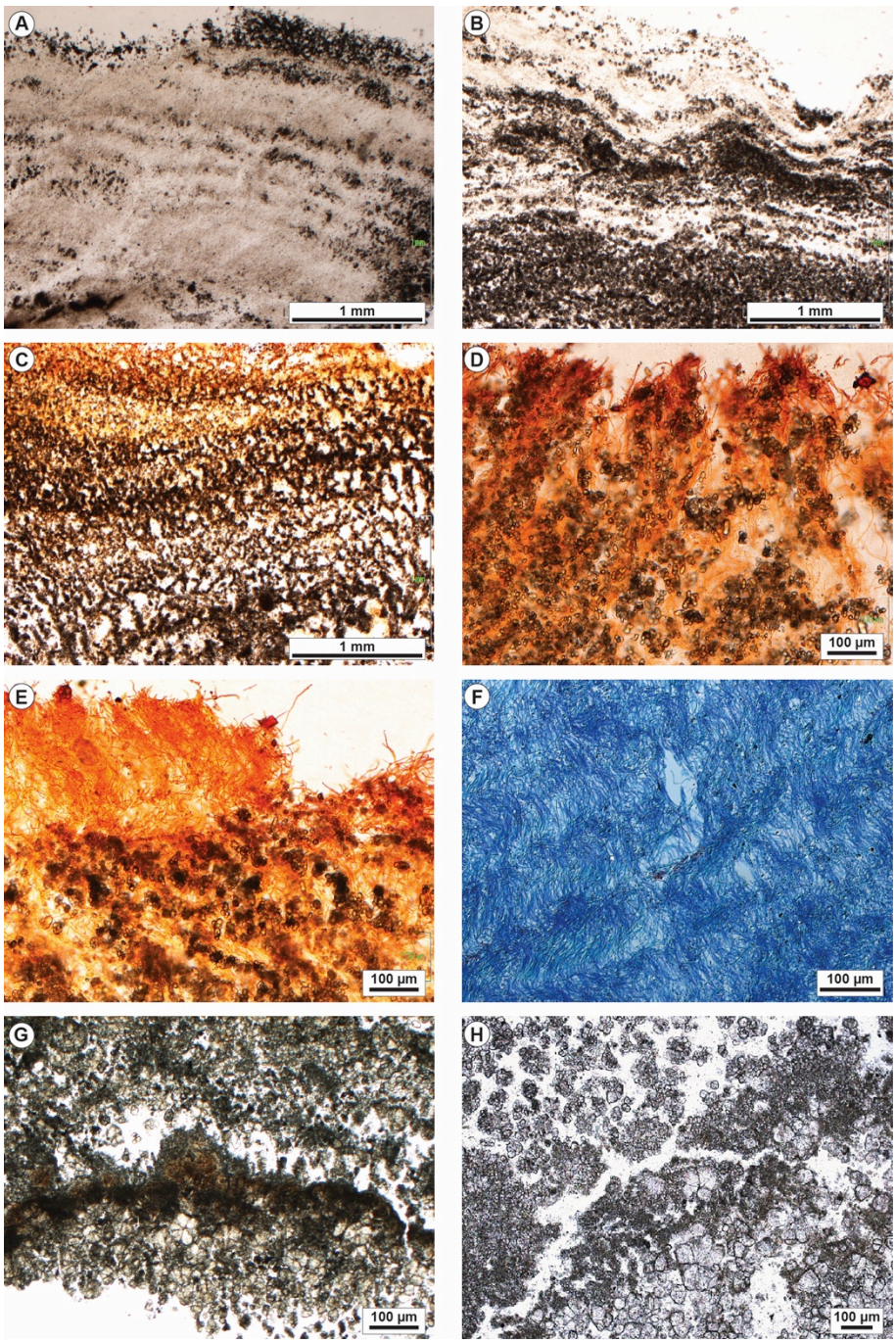

Figure S8. Gorello Waterfall (Saturnia) travertines from the rims and walls of the terraced slope system. A) Photomicrograph showing the micritic laminated boundstone with alternation of carbonate precipitates and microbial mat that acted as organic matter substrate for carbonate precipitation. B) Laminated boundstone showing the wavy lamination made of precipitated carbonate alternating with organic matter from the microbial mat. C) Calcein dyed laminated boundstone showing that carbonate crystals precipitated following the alveolar fabric of the biofilm EPS. D) Calcein dyed sample showing the microsparite crystals and spherulites precipitating in between the erect filamentous microbes making the outer layer of the microbial mat. E) Calcein dyed sample showing the erect filamentous microbes making the outer layer of the microbial mat with below micrite and microsparite precipitated following the spatial distribution of the filamentous microbes. F) Paraffin sample dyed with alcian blue showing the geometry of filamentous microbes in the microbial mats mimicked by the laminated carbonate precipitates. G) Laminated boundstone with microsparite/sparite spherulites and clotted peloidal micrite laminae. H) Framework made of microsparite/sparite spherulites and clotted peloidal micrite.

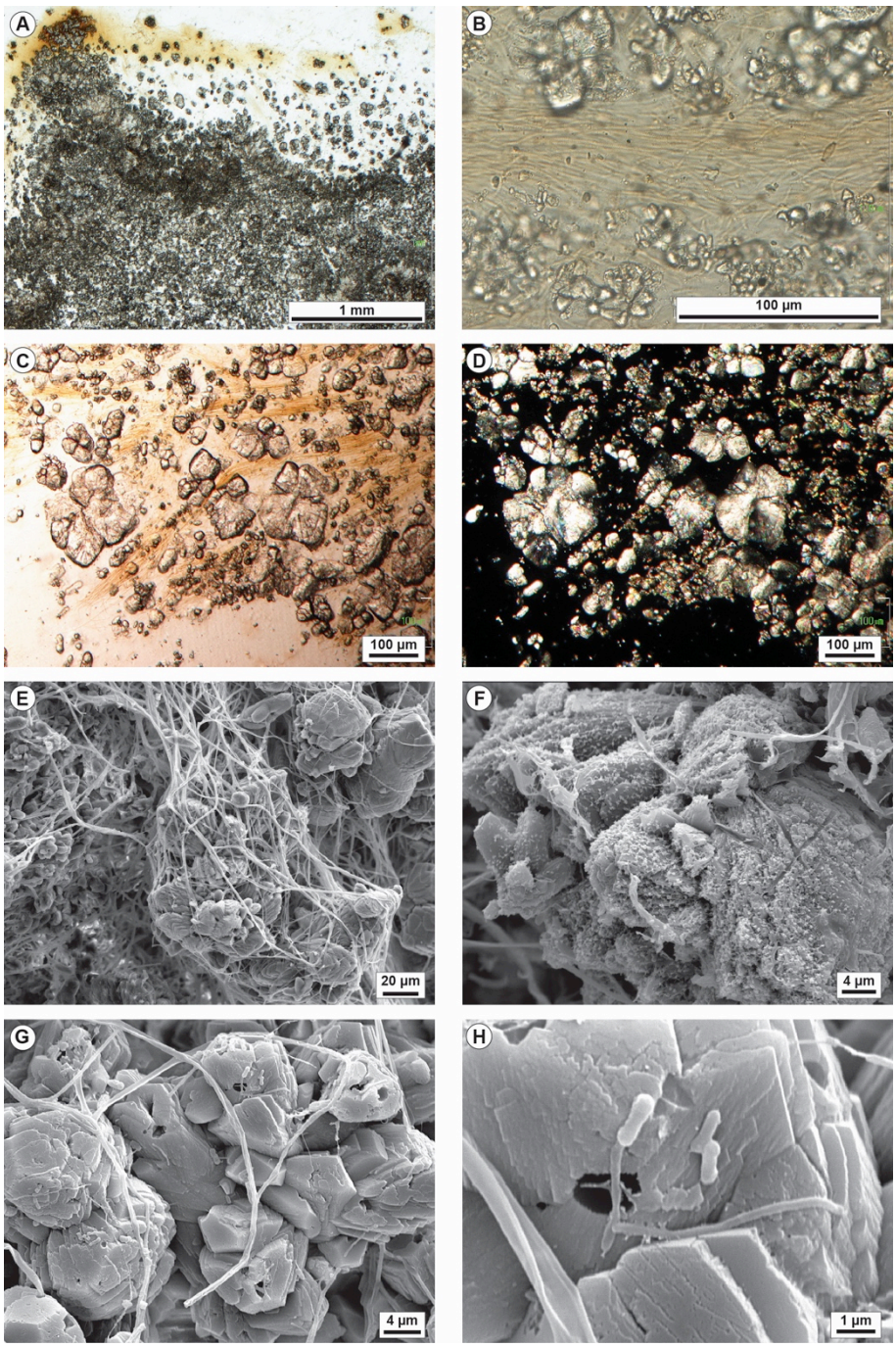

Figure S9. Petrographic and SEM images of the Gorello Waterfall (Saturnia) travertines from the rims and walls of the terraced slope system. A) Tetracycline dyed sample showing the framework of clotted peloidal micrite and microsparite spherulites overlain by the outer microbial mat. B) Close-up view in a tetracycline dyed sample showing microsparite spherulites alternating with microbial biofilm with dense concentration of filamentous microbes including *Spirulina* cyanobacteria. C) Microsparite to sparite spherulites floating within filamentous microbes. D) Crossed-polarizers image of microsparite/sparite spherulites showing the undulose extinction of the fan-shaped calcite crystals. E) SEM image showing dodecahedral calcite crystals forming aggregates and rosettes surrounded by filamentous microbes. F) SEM image of calcite crystals coated by mucilaginous organic matter, likely EPS, with tubular moulds related to the entombed filamentous microbes. G) Dodecahedral calcite crystals with tubular moulds related to the entrapped filamentous microbes and rod-shaped microbes. H) Close-up view of rod-shaped microbes with a dumbbell shape.

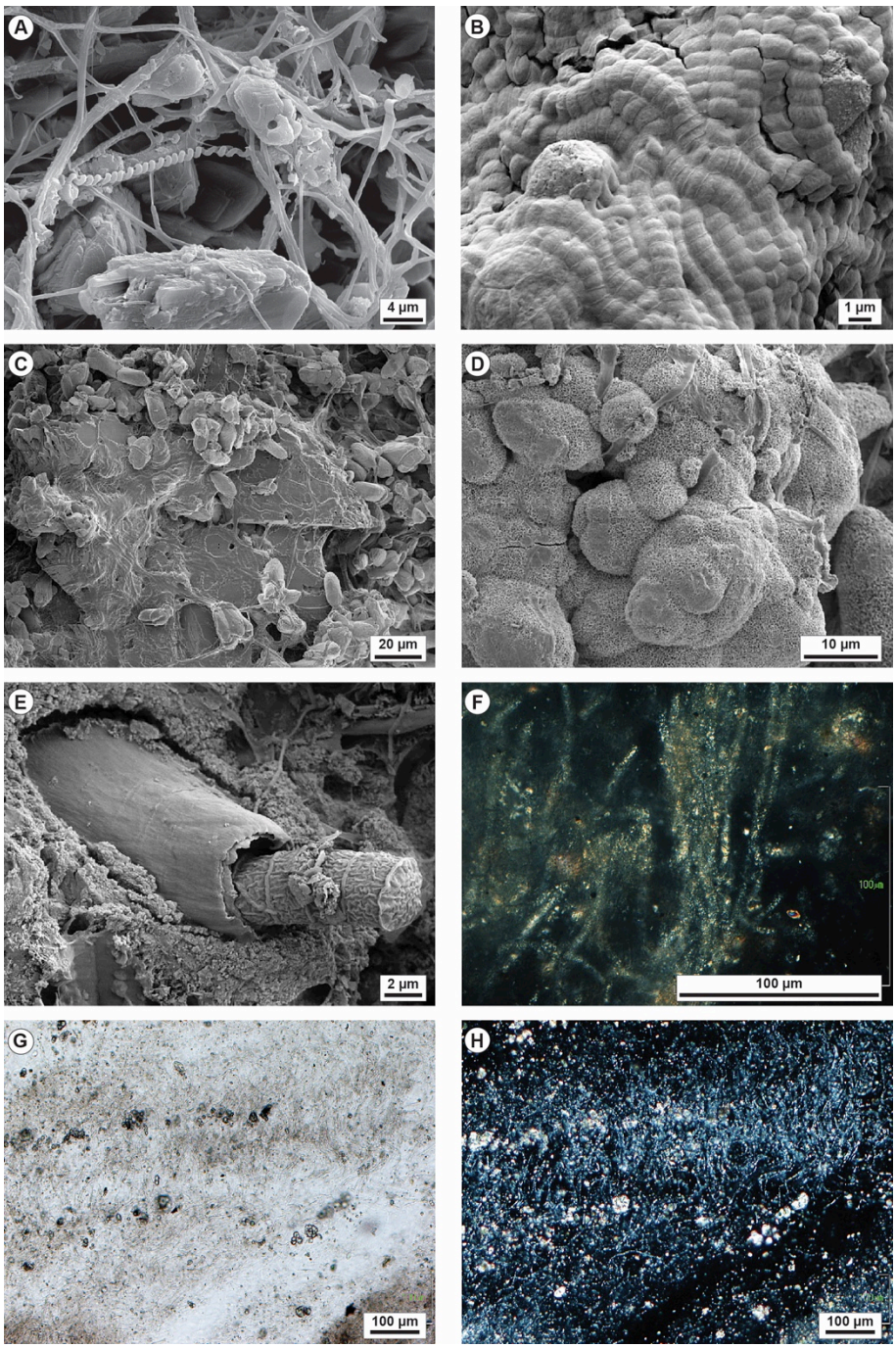

Figure S10. Petrographic and SEM images of the Gorello Waterfall (Saturnia) travertines from the rims and walls of the terraced slope system. A) SEM image showing calcite crystals surrounded by filamentous cyanobacteria including *Spirulina*. B) Segmented filamentous microbes probably belonging to *Phormidium*, *Oscillatoria* or *Fischerella* cyanobacteria. C) SEM image showing Ca phosphate crystals, probably apatite, coated by microsparite crystals, EPS and filamentous microbes with *Spirulina*. D) Spongy texture of phosphate coating the calcite crystals with a chemical composition of Ca and P through EDX analysis. E) Large segmented cyanobacteria with a thick sheath likely belonging to *Calothrix thermalis*. F) Crossed-polarizers image of large filamentous microbes probably belonging to the cyanobacteria *Calothrix* that show a birefringent internal filling material that could be an authigenic aluminum-silicate probably a clay mineral. G and H) Parallel and crossed polarizers photomicrographs of the microbial mat with erect filamentous microbes and sparse microsparite spherulites where the filamentous cyanobacteria are filled by aluminium-silicate material showing birefringence.

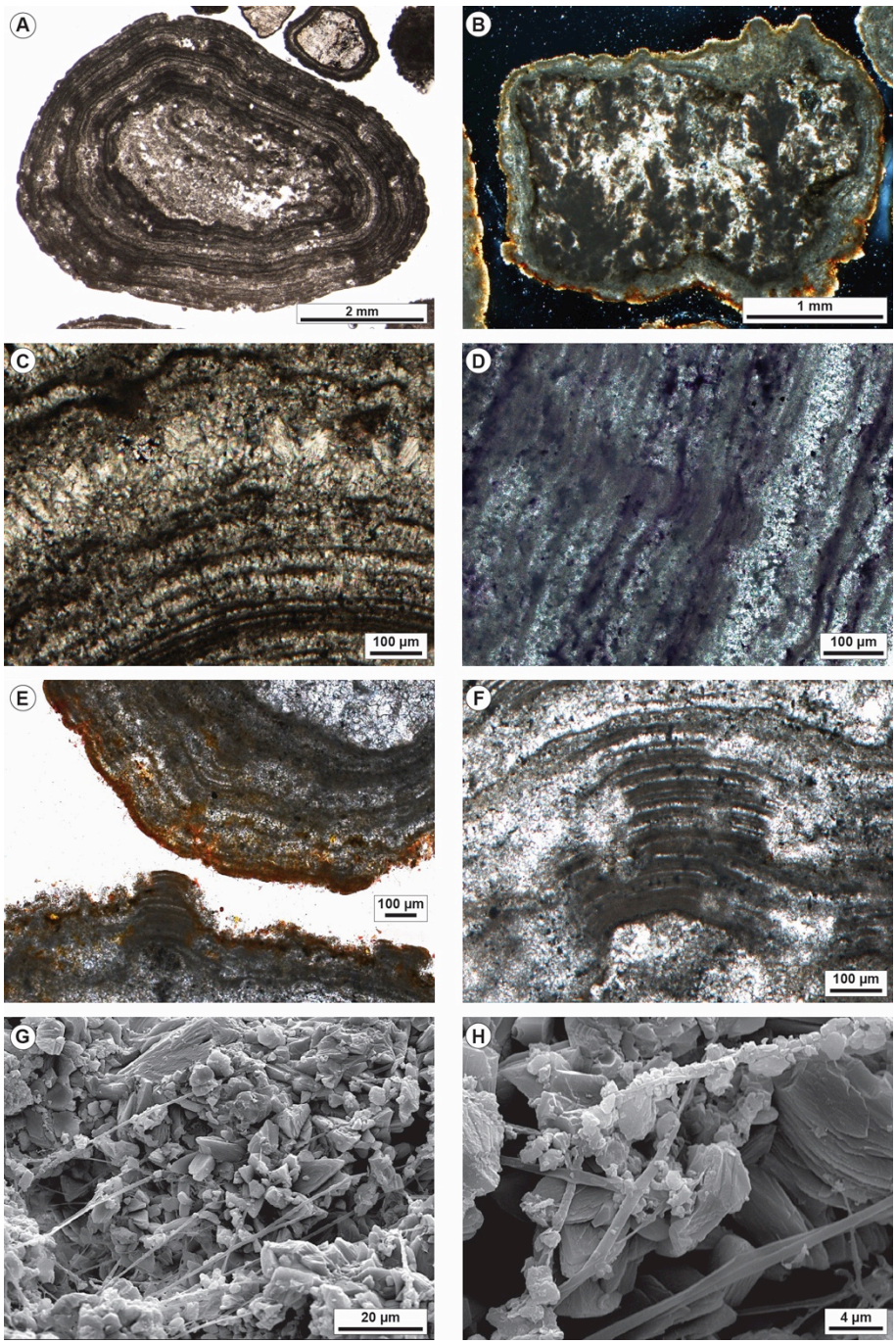

Figure S11. Petrographic and SEM images of the Gorello Waterfall (Saturnia) oncoids from the pools of the terraced slope system. A) Photomicrograph of oncoids with regular parallel undulated laminae made of micrite and microsparite and nuclei made of travertine intraclasts. B) Crossed polarizers image of an oncoid with the outer surface draped by tetracycline dyed microbial organic matter and nucleus made of travertine intraclast with clotted peloidal micrite dendrites surrounded by calcite spar. C) Crossed-polarizers image of oncoid laminae made of micrite alternating with palisades of bladed calcite crystals. D) Micritic and microsparitic laminae of oncoids containing organic matter as evidenced by toluidine dye. E) Outer portion of the cortex of two oncoids showing the microbial mat draping the outer surface as evidenced by calcein dye. The micritic laminae are locally eroded and truncated with organic matter infilling the microborings. F) Close-up view of truncated micritic laminae and microsparite replacing and filling the void left by removal of the micritic laminae. G) SEM image of calcite crystals forming the oncoid laminae with filamentous microbes extending perpendicular to the laminae surface. H) Filamentous microbes within the oncoid cortex encrusted by precipitated micrite.

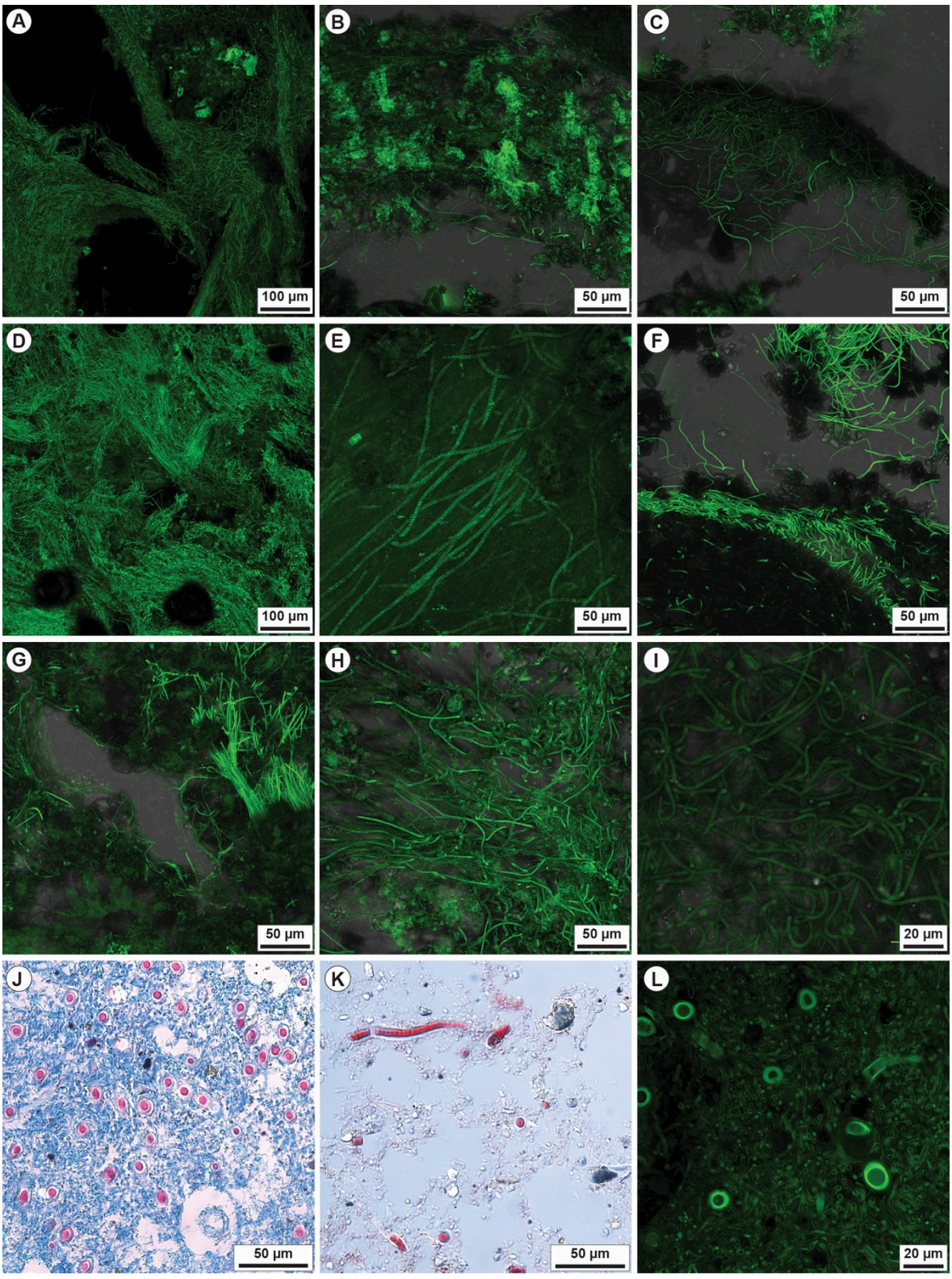
A
100 µm
B
50 µm
C
50 µm
D
100 µm
E
50 µm
F
50 µm
G
50 µm
H
50 µm
I
20 µm
J
50 µm
K
50 µm
L
20 µm

Figure S12 previous page. Confocal laser scanning microscope images of samples dyed with calcein from Bullicame (A-C), Bollore (D-F) and Gorello Waterfall (G-L). A) Sample from the Bullicame proximal channel showing the bundles of filamentous microbes forming the streamers. B-C) Sample from the Bullicame distal channel with abundant EPS and *Spirulina* filamentous cyanobacteria. D) Filamentous microbes from the calcified filamentous streamers sampled in the Bollore proximal channel. E) Bollore second vent channel with EPS embedding filamentous microbes including possible sulphide oxidizers and *Spirulina* cyanobacteria. F) Bollore distal channel with microbial mat dominated by *Spirulina* cyanobacteria. At the image top, calcite crystals are lined by green fluorescent organic matter. G) Gorello laminated boundstone with carbonate precipitates embedded in EPS and filamentous cyanobacteria including *Spirulina* and segmented forms. The porosity within the microbial mat lacks carbonate precipitates. H) Erect filamentous cyanobacteria alternating with prostrated filamentous microbes controlling the formation of lamination in the pool rim boundstone. I) Entangled filamentous cyanobacteria of the Gorello Waterfall microbial mat including also segmented specimens. J) Paraffin prepared sample stained with alcian blue and cell centre red staining (Kernechtrot) showing the blue network of filamentous cyanobacteria associated with larger size cyanobacteria with a thick sheath, probably *Calothrix thermalis*. Alcian blue is a polysaccharide stain characterising EPS with abundant COO- groups. K) Paraffin prepared sample stained with Masson-Goldener solution showing the longitudinal section and the segmented appearance of the larger size cyanobacteria inferred as *Calothrix*. L) Confocal laser scanning microscope image showing the cross-section of the thinner filamentous cyanobacteria and the sparse larger size putative *Calothrix* with thick sheath.

Table S1. Results of stable carbon and oxygen isotope analyses from the three travertine study sites.

Samples	$\delta^{13}C$ (‰ V-PDB)	$\delta^{18}O$ (‰ V-PDB)
Bullicame (Viterbo)		
Streamers		
BUL-A-18	5.4	-12.1
BUL-1	5.5	-11.6
BUL-1b	5.4	-11.6
Average (n = 3)	5.4	-11.8
Standard Deviation	0.1	0.3
Rafts and coated bubbles		
BUL-3A	7.3	-9.2
BUL-A-9R	7.2	-11.0
BUL-3B	7.5	-8.7
BUL-3C	7.4	-8.9
Average (n = 4)	7.3	-9.4
Standard Deviation	0.2	1.0
Coated reeds		
BUL-2B	6.8	-9.0
BUL-2A	6.7	-10.0
Average (n = 2)	6.7	-9.4
Standard Deviation	0.0	0.6
Bollore (Bagni San Filippo)		
Streamers		
BF-1.3d	4.2	-12.9
BF 1.3b	4.1	-12.8
BSF-GA1	4.4	-12.4
BSF-GA2	4.9	-12.4
BSF-GA3	4.8	-12.5
Average (n = 5)	4.5	-12.6
Standard Deviation	0.3	0.2
Rafts and coated bubbles		
BSF 1a	5.8	-11.4
BSF 1b	5.7	-11.4
BSF-GC-2	5.0	-12.6
BSF-GC-1	5.2	-12.5
BSF 14G	5.6	-11.6
BSF-GC	4.9	-12.5
BSF-R	5.1	-12.0
BSF-Rb	5.1	-12.2
Average (n = 8)	5.3	-12.0
Standard Deviation	0.3	0.5
Dendrites		
BSF GBa	4.8	-12.6

BSF-GBb	5.9	-12.1
Average (n = 2)	5.4	-12.4
Standard Deviation	0.8	0.4

Gorello Waterfalls (Saturnia)	$\delta^{13}C$ (‰ V-PDB)	$\delta^{18}O$ (‰ V-PDB)
Laminated boundstone rims and walls		
GOR-13	3.3	-8.3
GOR-14	3.1	-8.3
GOR-15	3.5	-8.2
GOR-16	2.7	-8.8
GOR-17	3.5	-8.3
GOR-18	2.9	-8.8
GOR-19	2.2	-8.9
SAT-3ox	2.6	-8.6
SAT-ox	2.9	-8.5
SAT-1ox	2.5	-8.6
SAT-3	2.6	-8.5
SAT-F1	3.0	-8.6
SAT-F2	3.0	-8.5
SAT-F3	3.0	-8.6
SAT-2b	2.5	-8.6
SAT-2ox	3.1	-8.5
SAT-1ox	3.0	-8.6
Average (n = 17)	2.9	-8.5
Standard Deviation	0.4	0.2
Coated grains (oncoids) in pools		
GOR-3	2.6	-8.5
GOR-4	2.8	-8.2
SAT-S2	2.6	-8.6
SAT-S1ox	2.7	-8.5
SAT-S2ox	2.7	-8.6
Average (n = 5)	2.7	-8.5
Standard Deviation	0.1	0.2
Rafts and coated bubbles		
GOR-2	2.2	-8.4
Coated reeds		
GOR-1	3.1	-8.2